I&EC research
Industrial & Engineering Chemistry Research

Article

Cite This: Ind. Eng. Chem. Res. XXXX, XXX, XXX−XXX

pubs.acs.org/IECR

A First Assessment on the Scale-Up Possibilities of Different Electrochemical Techniques for Lithium Isotopic Enrichment

Lautaro N. Acosta and Victoria Flexer*

Centro de Investigación y Desarrollo en Materiales Avanzados y Almacenamiento de Energía de Jujuy (CIDMEJu), CONICET, Universidad Nacional de Jujuy, Centro de Desarrollo Tecnológico General Savio, Av. Martijena s/n, 4612 Palpalá, Jujuy, Argentina

Supporting Information

ABSTRACT: Chemicals enriched in lithium isotopes are of paramount importance in the current nuclear fission technology, in future nuclear fusion technology, and in neutron detectors. Currently, lithium isotopes are obtained by using mercury amalgams, which is a nonenvironmentally friendly procedure. An interesting alternative is to take advantage of the electrochemical isotope effect. Here, we take, as the departure point, experimental data that were already reported for a prospective first stage of an electrochemical process, and we numerically simulate different scale-up possibilities. We calculate the minimum number of repetitive stages needed to reach a certain degree of isotopic enrichment. Second, we improve our simulations, considering that different operating conditions are used while keeping the same fundamental electrochemical process: a minimum of 145 stages are necessary to produce a sample with 90% enrichment in ^{6}Li. We conclude with a comparison on the different electrochemical technologies, in view of the complementary steps necessary for scaling up.

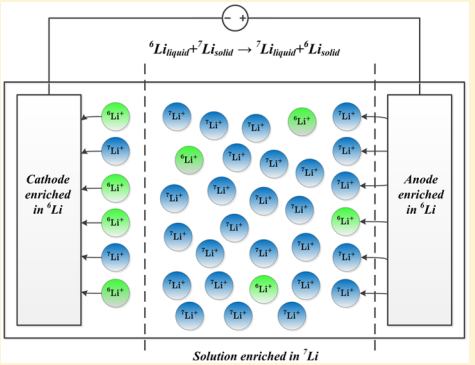

1. INTRODUCTION

Lithium has two naturally occurring isotopes, and both of them are stable: ^{6}Li and ^{7}Li, with natural abundances of 7.58% and 92.42%, respectively.[1] Although chemical properties are directly related to the electronic configuration of the atom, the mass difference between the isotope nuclei confer slightly different behavior to molecules and ions containing different isotopes of the same element. This phenomenon is known as the *isotope effect*.[2] Molecules or ions containing different isotopes of the same element are termed *isotopologues*.

It is of technological paramount importance to be able to produce materials with an enriched isotopic abundance, i.e., different from the natural abundance. The use of isotopes covers a wide variety of fields, ranging from radioactive tracers, nondestructive testing, radiotherapy in human medicine, nuclear fuels, molecules with substituted isotopes for mechanistic studies in chemistry and biology, and signature as tracer in environmental geochemistry.[3−8] Therefore, the isotopic separation of different elements—uranium, hydrogen, lithium, and iodine, among many others—is a widely studied research topic.

The different properties of isotopes of the same element, is what makes the isotope effect appealing, from a technological point of view. Interestingly, these differential properties are also what allows us to produce samples that are enriched in one isotope over the others, i.e., to partially separate isotopologues between two phases. The process of isotope separation bears certain similarities, from a technological point of view, with other separation process, such as distillation of hydrocarbons or liquid−liquid extraction of aromatic compounds. However, because of the chemical and physical similarities of the species involved, the degree of separation obtained in one stage is very low, rendering the entire separation process much more arduous.

In the specific case of lithium, the two stable isotopes display extreme values of cross section: 940 barns for ^{6}Li, vs 0.045 barns for ^{7}Li.[9] This nuclear property quantifies the effective area of collision and the interaction probability with other particles. Both lithium isotopes are employed in nuclear technology and research. ^{7}Li has been used for decades in nuclear fission reactors. Conversely, ^{6}Li is envisioned to have a paramount role in nuclear fusion reactors, a technology under development. Moreover, ^{6}Li is currently used in neutron detectors present in many high-end technological applications, such as use in satellites.

In addition to elements lighter than nuclear fuels, neutrons are also typical products in the reactor core where a nuclear fission reaction occurs.[10] If uncontrolled, scattered neutrons are dangerous, because they can trigger different unwanted nuclear reactions. Therefore, to absorb this radiation, a variety of *neutron poisons*, which are chemical substances with a high cross-sectional value, must be used. In pressurized water reactors, boric acid (3840 barn) is added to water to help

Received: April 16, 2018
Revised: June 20, 2018
Accepted: July 24, 2018
Published: July 24, 2018

DOI: 10.1021/acs.iecr.8b01640
Ind. Eng. Chem. Res. XXXX, XXX, XXX−XXX

control the reactivity of the core. To counteract the corrosive effect of boric acid, small quantities of ^{7}LiOH are added as a pH adjustor. It is important that added LiOH is heavily enriched in ^{7}Li (above 99.99% enrichment), which is highly transparent to neutrons, because of the very low cross-sectional value. On the other hand, ^{6}Li has a high cross-sectional value, and under neutron bombardment reacts to produce tritium, according to reaction 1:

$$^{6}\mathrm{Li} + n \rightarrow {}^{4}\mathrm{He} + {}^{3}\mathrm{T} \qquad (Q = 4.78\ \mathrm{MeV}) \tag{1}$$

Since tritium is radioactive, it is important that ^{6}Li is not present in pressurized water reactors.

Conversely, neutronic bombardment of ^{6}Li is the most common method to produce tritium in situ.[11] In the research of controlled nuclear fusion, tritium, together with deuterium, are part of the easiest reaction to develop a fusion process (eq 2):

$$^{2}\mathrm{D} + {}^{3}\mathrm{T} \rightarrow {}^{4}\mathrm{He} + n \qquad (Q = 14.1\ \mathrm{MeV}) \tag{2}$$

Deuterium is a stable isotope of hydrogen with natural abundance of 0.015%,[12] i.e., its availability is high. Conversely, tritium (^{3}T) is a radioactive isotope and naturally decays to ^{3}He, emitting beta radiation. Its natural abundance is at trace levels, with tritiated water having an abundance of $\sim 10^{-18}$, that of natural water.[11] For this reason, tritium must be produced in situ in nuclear fusion reactors, and reaction 1 is the easiest way to do this. Indeed, in prototype nuclear fusion reactors, the reactor core is supplied with a tritium breeding material, usually lithium silicates or titanates, that produce tritium through a nuclear reaction induced by neutron bombardment. For best space utilization of the breeding blanket and design considerations, it is necessary that the breeding material is enriched in ^{6}Li, between 30% and 90%.[13,14]

A large number of isotope separation methods for lithium have been tested.[15−17] Processes used for other isotopes, such as uranium or hydrogen, were tested for its application in lithium isotope separation. Among the possibilities, we find research articles that investigate molecular distillation in vacuum,[18] liquid−liquid extraction,[19−22] chemical exchange with different resins,[23−26] ion exchange chromatography,[27−30] zone melting and crystallization,[31,32] and separation by laser excitation.[33−36]

All these separation processes take advantage of the difference in some particular property between the isotopologues and, as a result achieve a variation in the isotopic composition after the aforementioned separation process. Depending on which technique is applied, the enrichment grade can vary in a relative wide range,[2] although the enrichment percentage is never higher than a one-digit figure. As we mentioned previously, the isotope enrichment of the final materials must be ∼99.99% in the case of ^{7}Li, and 30%−90% for the case of ^{6}Li. In view of this, regardless of the separation procedure, we can ensure that it is necessary to repeat the process several times in each case. This observation can be corroborated in different examples of industrial isotope separation.[37−40]

The current market of isotopically enriched ^{7}Li samples consists on the demand for pressurized water reactors and molten salt reactors. On the other hand, ^{6}Li-enriched samples are the base material for the synthesis of lithium silicates and titanates for tritium breeding blankets in experimental fusion reactors, such as DEMO and ITER, and different types of neutron detectors. Unfortunately, ^{6}Li is also used in the production of nuclear weapons, which is an application that we certainly do not encourage. The important market of enriched materials in ^{6}Li and ^{7}Li has led to research for the development of several methods of enrichment. In the particular case of the United States, the Oak Ridge Y12 plant tested three different enrichment processes: electrically driven chemical exchange (ELEX), organic exchange (OREX), and column chemical exchange (COLEX).[41] Of these three alternatives, the only one that achieved industrial scale was the COLEX process. Its operation consists of a cascade of stages within an exchange column where the lithium isotopes are redistributed between an aqueous solution of LiOH and Li−Hg amalgam that flows counter-currently. ^{6}Li has greater affinity for the mercury amalgam, while the ^{7}Li isotope is concentrated into the aqueous solution. The basis of both the fundamental chemistry and the engineering of the industrial process was reviewed by Okuyama et al.[42] and Fujie et al.[43] The isotopic exchange reaction is depicted in reaction 3.

$$^{7}\mathrm{LiHg} + {}^{6}\mathrm{LiOH}_{(aq)} \leftrightarrow {}^{6}\mathrm{LiHg} + {}^{7}\mathrm{LiOH}_{(aq)} \tag{3}$$

The enrichment process was conducted in the Oak Ridge Y12 plant between 1954 and 1963, and, during this period, the domestic demand was supplied and a large stockpile was accumulated. Because of the hazard to employ large amounts of amalgam during the separation process (∼10 890 tonnes of mercury), this plant was closed. An extensive report published by Brooks et al.[41] details the magnitude of the environmental impact by the continuous operation of this enrichment method. Russia and China still produce ^{6}Li and ^{7}Li via the COLEX process. However, the negative environmental impact of employing large amounts of mercury presents the challenge to perform research on alternative methods for isotope separation.

Electrochemistry provides clean solutions for many industrial processes, and the isotope effect is also present in fundamental electrochemical phenomena. Several researchers have explored different possibilities to use electrochemistry to produce lithium samples enriched in either of the isotopes, including electrodeposition, intercalation in different materials, and electrodialysis, among others.[44−55] In previously reported work, the enrichment grade after a single stage is low and, therefore, the isotopic composition of either of the phases is still unsatisfactory for the produced samples to be employed in any of the above-mentioned applications. All the work published so far is clearly of fundamental nature, i.e., electrochemical cells are of very small volume and only a single enrichment stage is reported. There is a clear lack of analysis on the prospective scale-up possibilities of the proposed fundamental electrochemical reactions. In this Article, we calculate the number of stages that would be needed to reach the desired and final enrichment grade, for the different electrochemical methodologies proposed so far. We also calculate the energy consumption and the costs of the entire enrichment process until the desired enrichment grade is attained. These calculations allow us to start bridging the gap between molecular-level electrochemical separation and large-scale chemical production.

2. THEORY AND METHODOLOGY

As in any separation process, the efficiency of the isotopic enrichment is expressed through a separation factor that

DOI: 10.1021/acs.iecr.8b01640
Ind. Eng. Chem. Res. XXXX, XXX, XXX−XXX

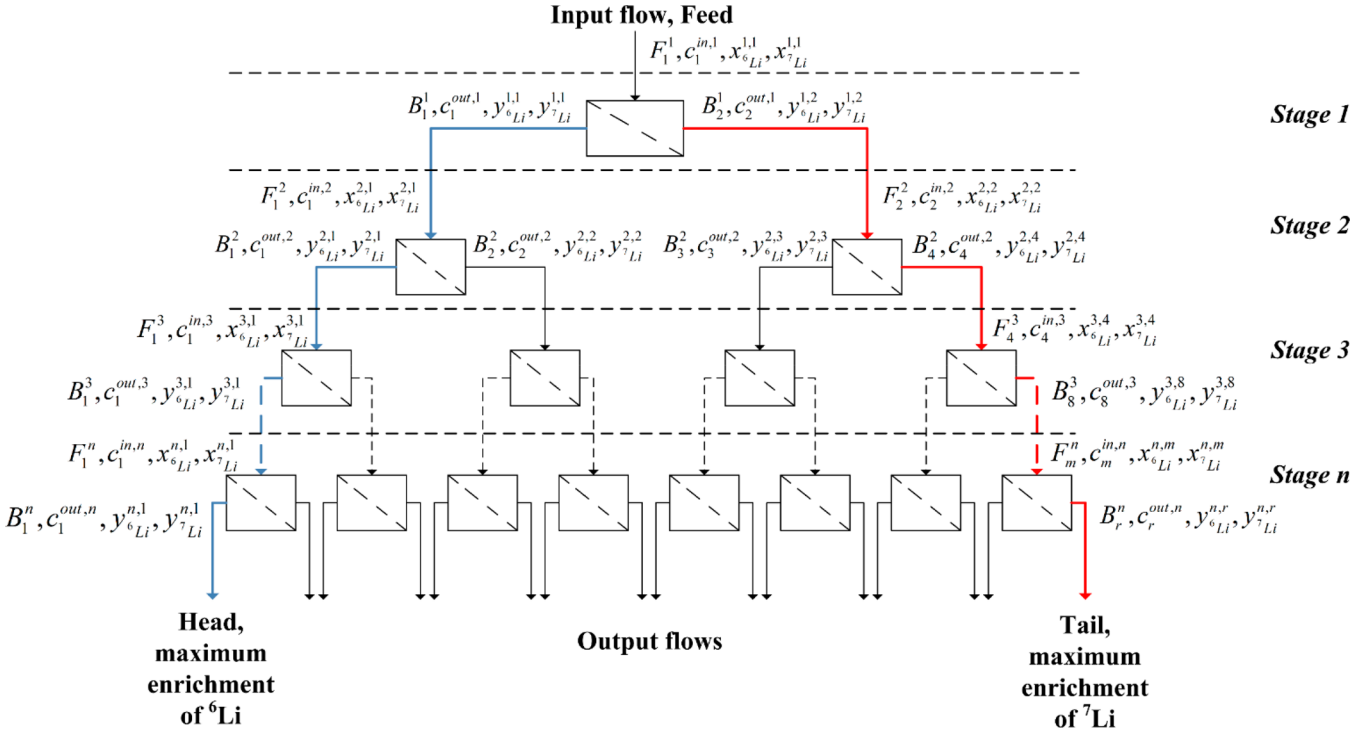

Figure 1. Generic serial process for lithium isotope separation formed by n stages with units in parallel.

quantifies the distribution of the species of interest between two phases (enriched and depleted phase, respectively). The most important parameter to characterize a separation process is the single-stage separation coefficient, denoted as α and referenced as the *alpha* factor, which indicates the degree of fractionation that is attained. By definition, this is equal to the ratio of isotopic abundance in each phase after one enrichment stage:

$$\alpha_{^6\mathrm{Li}/^7\mathrm{Li}} = \frac{\left(\frac{x_{^6\mathrm{Li}}}{x_{^7\mathrm{Li}}}\right)_{\mathrm{E}}}{\left(\frac{x_{^6\mathrm{Li}}}{x_{^7\mathrm{Li}}}\right)_{\mathrm{D}}} \tag{4}$$

where $x_{^6\mathrm{Li}}$ and $x_{^7\mathrm{Li}}$ denote the isotopic fractions of ^{6}Li and ^{7}Li respectively. The subscripts E and D represent the enriched phase (head) and the depleted phase (tail), respectively. Because values for all reported methods so far are very close to unity, another practical way to present this information is the enrichment factor (ε):

$$\varepsilon_{^6\mathrm{Li}/^7\mathrm{Li}} = \alpha_{^6\mathrm{Li}/^7\mathrm{Li}} - 1 \tag{5}$$

Different processes that involve species exchange or a redox reaction are performed in each separation unit. Mass balances for these systems are focused on the atomic species (in this case, the lithium isotopes). Consequently, the mass balance equations become conservation equations, because the generation terms are nonexistent.

$$\{\cancel{accumulation}\} = \{input\} - \{output\} + \{\cancel{generation}\} \tag{6}$$

$$\{input\ species\ j\} = \{output\ species\ j\} \tag{7}$$

At the beginning of the process, the lithium source displays the natural isotopic abundance. The mass balance for the continuous process is described by eqs 8 and 9:

$$\sum_{i=1}^{m} F_i^a \cdot c_i^{\mathrm{in},a} = \sum_{j=1}^{r} B_j^a \cdot c_j^{\mathrm{out},a} \qquad (a = 1, 2, 3, ..., n) \tag{8}$$

$$\sum_{i=1}^{m} F_i^a \cdot c_i^{\mathrm{in},a} \cdot x_{\mathrm{A}}^{a,i} = \sum_{j=1}^{r} B_j^a \cdot c_j^{\mathrm{out},a} \cdot y_{\mathrm{A}}^{a,j} \tag{9}$$

Equations 8 and 9 hold true at each individual stage. F represents the input (feed) fluxes. In the general case, there is a total of m input fluxes. B represents the number of output fluxes (head and tail) of each stage; and r denotes their total number. Note that $r \geq m$ in the general case. When there is only a single feed in the process, $r > m$, because the isotopes must be redistributed in at least two phases. Superscript a represents the stage number between 1 and n, the final stage. In the processes described in sections 3.1−3.6, there is a single feed, and two output fluxes, the head (which is enriched in ^{6}Li), and the tail (which is slightly depleted in ^{6}Li, if compared to the feed of that same stage). In the process described in section 3.7, there are two input fluxes and two output fluxes.

In eqs 8 and 9, c^{in} represents the lithium concentrations (all isotopes together) in each input flux (feed) and, c^{out} represents the lithium concentrations in each output flux (head and tail). x_{A}^j and y_{A}^j represent the isotopic fractions of isotope A in the different input and output fluxes, respectively. Furthermore, there is the restriction that, for each element, the sum of all isotopic fractions, in either the head, the tail, or the feed, must be equal to one:

for the feed solution:

$$x_{^6\mathrm{Li}}^1 + x_{^7\mathrm{Li}}^1 = 1 \tag{10}$$

for the head:

$$y_{^6\mathrm{Li}}^1 + y_{^7\mathrm{Li}}^1 = 1 \tag{11}$$

DOI: 10.1021/acs.iecr.8b01640
Ind. Eng. Chem. Res. XXXX, XXX, XXX−XXX

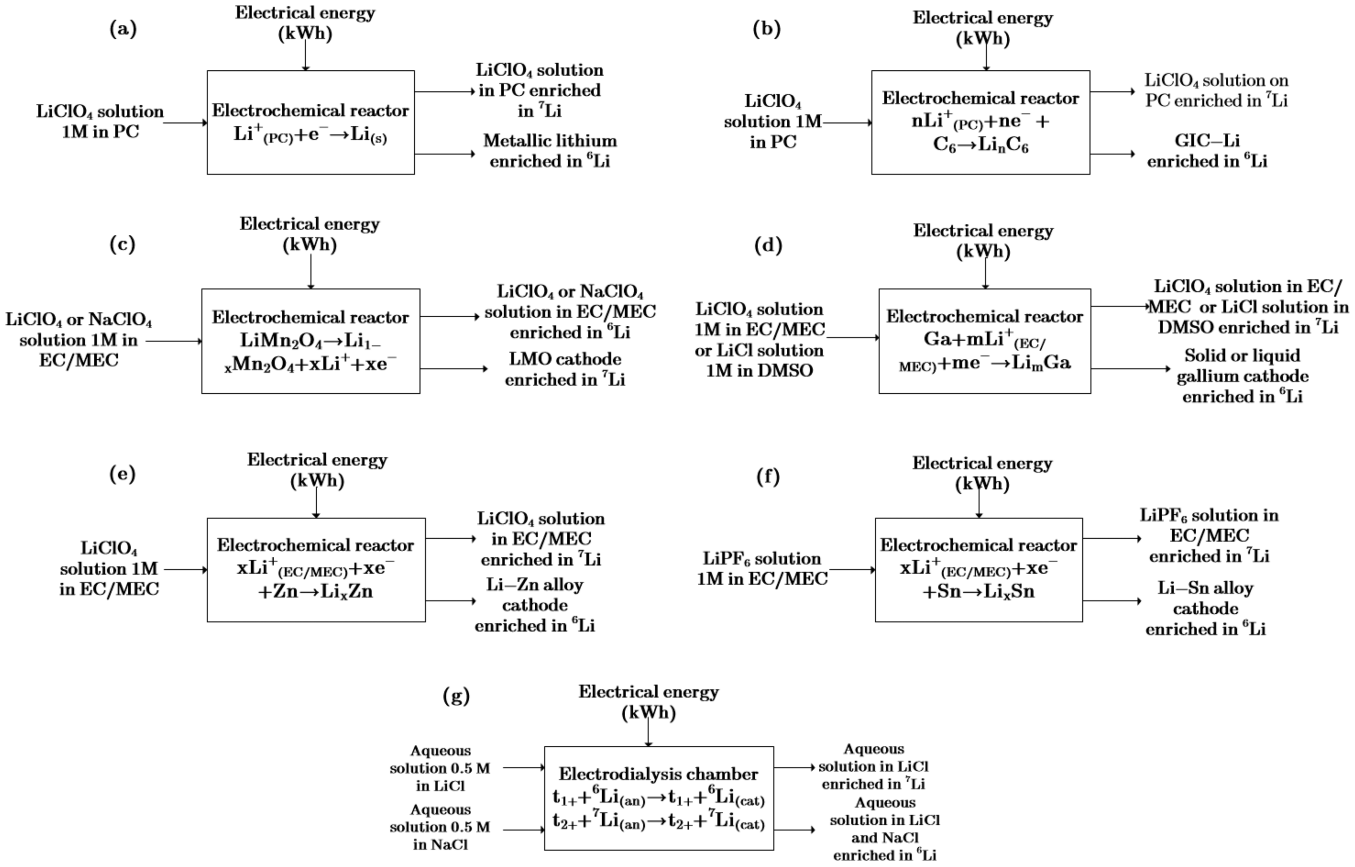

Figure 2. Input−output diagrams for all electrochemical system for lithium isotope separation discussed in the text: (a) lithium electrodeposition on nickel electrode; (b) electrochemical lithium intercalation into graphite; (c) delithiation of LMO electrode in organic solution; (d) electrochemical lithium insertion into liquid or solid gallium; (e) electrochemical lithium insertion into zinc; (f) electrochemical lithium insertion into tin; and (g) electrodialysis through an organic membrane embedded in ionic liquid.

for the tail:

$$y_{^6\mathrm{Li}}^2 + y_{^7\mathrm{Li}}^2 = 1 \tag{12}$$

Fluxes, concentrations, and isotopic fractions are shown in Figure 1. The last important piece of information is the enrichment grade between stages, i.e., the difference in the isotopic fraction between stages n and $n-1$. This is calculated using eq 13:

$$\Delta x_{^6\mathrm{Li}} = x_{^6\mathrm{Li}}^{n} - x_{^6\mathrm{Li}}^{n-1} \tag{13}$$

We aim to calculate the total number of stages that are needed for an overall process to reach a certain enrichment grade. However, we cannot ignore the fact that, for every single stage, the head and tail have different characteristics than the feed.

Taking as a departure point the natural isotope abundance, and the α factor previously reported, eqs 4−13 can be used to build an equation system that allows us to obtain the proportion of light and heavy isotopes in every phase after the enrichment process: $x_{^6\mathrm{Li}}^{\mathrm{solid}}$, $x_{^7\mathrm{Li}}^{\mathrm{solid}}$, $x_{^6\mathrm{Li}}^{\mathrm{liquid}}$, and $x_{^7\mathrm{Li}}^{\mathrm{liquid}}$, for any of the processes described in sections 3.1−3.7. The resulting isotopic fractions in the enriched phase (for example, the solid in processes described in sections 3.1, 3.2, 3.4, and 3.6) are fed as the feed values in the next stage (output isotopic fractions of stage n, are the feed isotopic fractions in stage $n+1$). In this way, we build a hypothetical multistage configuration to reach a desired enrichment value. This sequence is repeated, using eqs 4−13, by an iterative loop written in Matlab until the finalizing condition is fulfilled. The finalizing condition is a specific isotopic fraction (for example, 0.9 for ^{6}Li). Each time that the cycle is completed, a support array saves the data to plot the enrichment curve through the entire process and the variation of the isotopic fractions between consecutives stages.

We started our work by making a literature search of published articles where different electrochemical methods have been proposed for the separation of ^{6}Li and ^{7}Li isotopes. The original experimental data was used to calculate the enrichment grade for every flux in a multistage process. Beyond the mathematical formulas, the algorithm is fed with data from already-published scientific articles (initial solution concentration, volume, isotope separation factor, total charge delivered, etc.). Figure 1 shows the topology of the separation units. The scheduling is dependent on the operation mode, either batch or serial, and the complexity increases with the number of separation stages. The typical serial process from Figure 1 displays a variety of fluxes with different compositions.

Calculations were performed under the following assumptions:

(1) The reported enrichment factor (α) for a first stage of a given enrichment process starting with the natural isotopic abundance remains constant for the following stages; i.e., we assume that the α factor remains unchanged through the different stages, even though, for these successive stages, the departure isotopic ratios

DOI: 10.1021/acs.iecr.8b01640
Ind. Eng. Chem. Res. XXXX, XXX, XXX−XXX

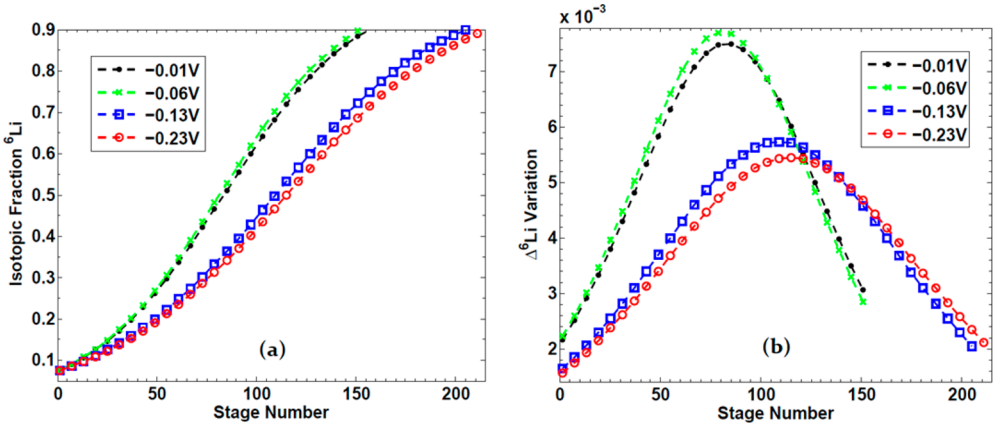

Figure 3. Simulation results for the electrodeposition of lithium on a nickel electrode: (a) enrichment curve per stage and (b) ^{6}Li isotopic fraction variation per stage.

Table 1. Summary of Optimal Operating Conditions and Reported Results for Coulombic Efficiencies, As Reported in the Original Articles[a]

			Stages for Enrichment until Composition in ^{6}Li Reaches							
method	operation conditions[b]	total charge per stage (C)	30%	90%	cut (Li transferred to enriched phase (%))	energy consumption[c] (Wh g^{-1})	total cost (US$ g^{-1})	Coulombic efficiency (%)	temperature (°C)	ref
electrodeposition	CV	0.1	54	153	1.99×10^{-3}	6200	1.09	33	25	44
intercalation into graphite	CC/CV	54.5	69	194	1.63	2700	0.47	87	25	45
delithiation of LMO	CC/CV	3.9	80	224	28.27	5920	1.03	61	25	46
insertion into liquid gallium	CC/CV	59.4	58	163	5.30	2290	0.40	81	50	47,48
insertion into Zn	CC/CV	56.3	79	223	6.73	2520	0.44	103.5	25	49
insertion into Sn	CC/CV	28.1	114	323	1.83	6640	1.16	64	25	50
electrodialysis	CC	5.6×10^{-4}	7	16	1.70×10^{-4}	PDNA[d]	PDNA[d]	NR[e]	NR[e]	51,52

[a]The table also gathers our calculations for energy consumption, cost, and the minimum number of stages needed for each technique to reach both 30% and 90% isotopic enrichment in ^{6}Li. Calculations for costs and duration take into account the enrichment steps only, omitting all side processes, such as regeneration of the departing phase. [b]CV = constant voltage; CC = constant current. [c]Energy consumption for intercalation techniques into graphite, Ga, Zn, Sn and delithiation of LMO are only approximate, since we do not have the original voltage data to integrate the energy consumption at a varying potential point by point. [d]PDNA = Potential data not provided to perform calculation. [e]NR = not reported.

differ considerably from previously tested concentrations.

(2) We suppose a serial process for the electrochemical process analyzed, without recirculation of streams or parallel units.

(3) Because of the separation process, we obtain two outputs (head and tail) in which the initial flux is distributed but differ in the total mass from the feed. However, we assume it is possible to retrieve these variables to their initial values automatically: mass and total Li^+ concentration, $[^6Li^+] + [^7Li^+]$, of the feed in stage 1. With this assumption, we avoid any effect of the feed concentration, i.e., we keep the total Li^+ concentration constant throughout the entire process. In a real industrial system, recirculation and the use of several units in parallel allows this to be done, but a precise calculation of such an arrangement is beyond the scope of this work.

3. RESULTS

3.1. Electrodeposition of Metallic Lithium. Black et al. tested the electroplating of metallic lithium on a nickel electrode from organic solutions.[44] The authors reported results for a 1 M solution of $LiClO_4$ in anhydrous propylene carbonate (PC). The experimental results show that, effectively, an isotopic enrichment in the resulting phases can be produced. The lightest isotope is preferentially partitioned into the deposited metal, while the heavy isotope remains in the stock solution.

The reaction is performed in a closed system, and Figure 2a shows the feed, the head and tail of a unit separation. Figure 3a shows our calculations for the enrichment curves for the metal phase. The figure plots the isotopic fraction reached versus the number of repetition of the isotopic separation (stages) for the different experimental conditions that were previously reported.[44] The simulations were run until a maximum isotopic enrichment of 90% is reached, which is the maximum recommended value for ^{6}Li content for breeding materials in

DOI: 10.1021/acs.iecr.8b01640
Ind. Eng. Chem. Res. XXXX, XXX, XXX−XXX

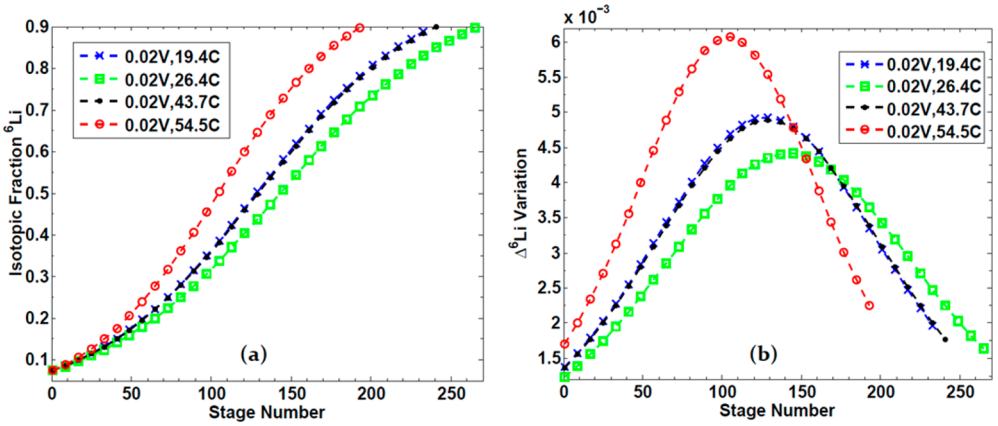

Figure 4. Simulation results for the electrochemical intercalation of lithium into graphite: (a) enrichment curve per stage and (b) ^{6}Li isotopic fraction variation per stage.

nuclear fusion technology. The original experiments were performed in chronoamperometry mode, applying different constant overpotential values between 0.01 V and 0.23 V. The total charge delivered in all cases was 0.1 C, which is a value that corresponds to a conversion of 0.0047% of the total Li ions present in solution. The reported Coulombic efficiency of the deposition process is quite low, between 31% and 46% (higher for the higher overpotential values), meaning that a parallel reaction is occurring, most likely solvent decomposition. Table S1 in the Supporting Information summarizes the results of our simulations for all the different experimental conditions reported in the original article. Figure 3b depicts the isotopic difference through the entire process.

Although the electroplating of lithium has only been reported for laboratory scale, it is interesting to highlight that the electrodeposition of metals on cathode surfaces is a very well-known process at industrial scale, and much previous expertise might be collected and extrapolated if we were to try to upscale this process.[56] Interestingly, metallic lithium is currently produced by an electrowinning process, although not from an organic solution, but from an eutectic melt of LiCl–KCl.[57] That electrolysis process operates between 6 V and 9 V and with an energy consumption of 35–40 kWh kg^{-1} Li, a value similar to the present case (6200 kWh kg^{-1} Li for 153 stages, i.e., on average, 40 kWh kg^{-1} Li per stage; see Table 1), where the authors worked at a lower voltage, albeit with a much lower Coulombic efficiency. Several references support the assumption of the independence of the electrochemical isotope effect, with regard to the extent of reaction.[58] The isotope fractionation remains constant, provided the reservoir composition does not present significant evolution. Therefore, it would be interesting to study the evolution of this reaction beyond the deposition of only 0.0047% of the feed.

3.2. Electrochemical Intercalation of Lithium into Graphite. Graphite intercalation compounds (GICs) are layered structures that allow for the electrochemical insertion of lithium or other elements into graphite. In the electrochemical insertion, lithium remains always in the +1 redox state, while carbon is reduced upon insertion of lithium. Graphite intercalated with lithium is the material of choice in anodes in modern lithium-ion rechargeable batteries.[59]

$$n\mathrm{Li}^+ + n\mathrm{e}^- + \mathrm{C}_6 \leftrightarrow \mathrm{Li}_n\mathrm{C}_6 \qquad (14)$$

Yanase et al.[45] studied the charge–discharge process of these electrodes as a possible technique for lithium isotope separation. Figure 2b is a schematic of the isotope redistribution in the two phases. This process consists in a closed system where the initial solution becomes enriched in ^{7}Li, while Li$^+$ ions are inserted into the graphite electrode, which is enriched in ^{6}Li at the end of the process. The process is analogous to the recharge of a lithium-ion battery, i.e., a graphite electrode operates as a cathode where the Li$^+$ ions are inserted. The solution phase was a 1 M solution of $LiClO_4$ in a mix of ethylene carbonate (EC) and methylethyl carbonate (MEC).

The intercalation procedure was first performed in constant current regime, until a set potential was reached, and it was then followed by a constant voltage regime. The process was tested for different set potentials, and for different total circulated charge. The experimental α value range was 1.007–1.025, depending on the set voltage and current values. Figure 4a is a plot of our simulations for the different experimental conditions versus the number of stages where the process is repeated. Figure 4b is a plot of the isotopic difference versus the number of stages. It is interesting to note that several operating conditions, albeit being very different, show extremely similar behaviors. It is also important to notice that, upon the choice of operating conditions, it might be possible to finish the overall enrichment process for very distinctive total number of repetitive stages: 175 total number of stages if operating at 0.02 V and 54.5 C, vs 320 total number of stages if operating at 0.07 V and 11.8 C. Table S2 in the Supporting Information summarizes the results of our simulations for all the different experimental conditions reported in the original article.

The analysis of the reported experimental data suggests correlation, to some extent, between the separation factor (α) and the stoichiometric number m in the formulas Li_mC. The authors observed that the greater the amount of lithium intercalated in graphite, the larger the isotopic fractionation, although the correlation is not perfect, and there is quite a large dispersion in the original data points.[45] This suggests the possibility to improve the isotopic separation efficiency, while simultaneously recovering a larger absolute amount of lithium into the graphite, which is a most interesting possibility in the perspective of an industrial scaleup. Also interesting from the perspective of a scale-up process is the fact that the intercalation of lithium into graphite is a very well-known process, because of the lithium-ion battery industry.

DOI: 10.1021/acs.iecr.8b01640
Ind. Eng. Chem. Res. XXXX, XXX, XXX–XXX

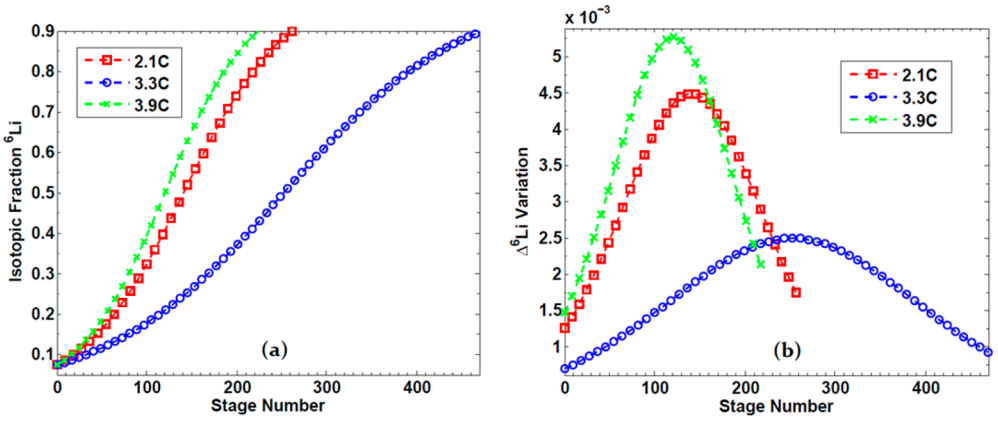

Figure 5. Simulation results for the delithiation of LMO electrode: (a) enrichment curve per stage and (b) ^{6}Li isotopic fraction variation per stage.

Interestingly, the authors also analyzed the possible source of the isotope effect.[45,60] Their most important assumption is that this originates from the equilibrium isotope effect on the overall reaction, i.e., the solvation−desolvation process of lithium ions near the electrode surface, and the reduction of graphite upon intercalation of lithium ions. Both events are affected by the presence of the solid electrolyte interface (SEI) that presents lithium ion conductivity and allows for the intercalation through this surface film.

3.3. Lithium Release from Lithium Manganese Oxide (LMO) Electrode. Okano et al.[46] proposed a technique also inspired in the current lithium-ion battery technology. However, this work was based on current cathodes for lithium-ion rechargeable batteries, instead of anodes.[61] Moreover, in the work proposed, the reaction that is responsible for lithium isotopic enrichment is the lithium deinsertion reaction from the solid structure, i.e., the passage from the solid phase to the solution phase of lithium atoms. The electrode material studied is a lithium manganese oxide (LMO) spinel, as depicted in eq 15:

$$LiMn_2O_4 \leftrightarrow Li_{1-x}Mn_2O_4 + xLi^+ + xe^- \quad (15)$$

The authors also worked with the same solvent mixture as in section 3.2.

Figure 2c depicts an in−out diagram of the proposed process. Because Li^+ ions are being deinserted from the LMO structure, in practice, the process is analogous to the charging of the cathode of a lithium-ion battery. The lithium release from $LiMn_2O_4$ is performed first in constant current mode, until reaching a predetermined voltage difference value. From this point, the ion release is carried out at constant voltage mode until the desired total electric charge reaches the predetermined value.

For our analyses of the total number of stages needed to enrich samples, we only considered four of the experimental conditions tested by Okano et al. The runs considered are those that correspond to 2.07, 3.27, 3.90, and 4.16 C of total charge delivered, and include experiments with and without lithium in the electrolyte. The resulting enrichment curves for the process are depicted in Figure 5a, together with those for the isotopic difference of the phase enriched in ^{6}Li in Figure 5b.

We can observe a large dispersion in the enrichment curves (see Table S3 in the Supporting Information), because of the wide range of α values. It is interesting to note that, depending on the operating conditions of the process, it is possible to finish the isotopic enrichment to the desired 90% ^{6}Li content in less than half of the total number of stages, when comparing the two most extreme conditions. We know that, generally, the heavy isotope is preferentially partitioned into the phase with stiffer chemical bonds.[2] If lithium atoms are tightly constrained into the spinel structure, it is possible that the bonds in the solvated sphere may be weaker, and this would explain the preferential partition of the heavy isotope into the electrode. The observed isotopic fractionation is also originated in the equilibrium reaction on the solution/electrode interface, and the partition constant determinates the isotope composition of both phases.

Interestingly, the authors work with a two-electrode configuration system, i.e., in the absence of a reference electrode, which means that the voltage difference is referred to the counter electrode. Moreover, the absence of a reference electrode is much more amenable to scaling-up possibilities. However, the fact that the departing material in each stage is a solid (LMO) makes it more difficult to envision how to prepare a new solid enriched in one of the isotopes to use as a new phase to be further enriched. One possibility would be to insert Li^+ into a $Li_xMn_2O_4$ with x values very close to zero.

In addition, the authors propose to use a graphite counter electrode to which a negative potential is applied, i.e., Li^+ will be inserted into the graphite. We have observed that, above that potential, this insertion will provoke an isotopic enrichment of ^{7}Li in the liquid phase, i.e., exactly the opposite from the desired effect (enrichment of ^{7}Li in the LMO phase). It is yet to be established whether another reaction at the counter electrode, and/or the use of some sort of separator (impermeable to Li^+ ions), would increment the α factor for lithium. Table S3 in the Supporting Information summarize all our results for the simulations as well as representative data from the original work.

3.4. Electrochemical Insertion of Lithium into Gallium. Zenzai et al. proposed the electrochemical insertion of lithium into, alternatively, solid[47] or liquid gallium.[48] Because the melting point for gallium (29.76 °C)[62] is very close to room temperature, it would be technologically easy to work in either of the aggregation states. These systems are a new possibility for lithium isotope separation, generated by the possibility to prepare lithium−gallium alloys, with formulas up to Li_2Ga at room temperature, i.e., gallium is capable of inserting three times more lithium in molar ratio than graphite, or almost twice more lithium in mass ratio, albeit at a much

DOI: 10.1021/acs.iecr.8b01640
Ind. Eng. Chem. Res. XXXX, XXX, XXX−XXX

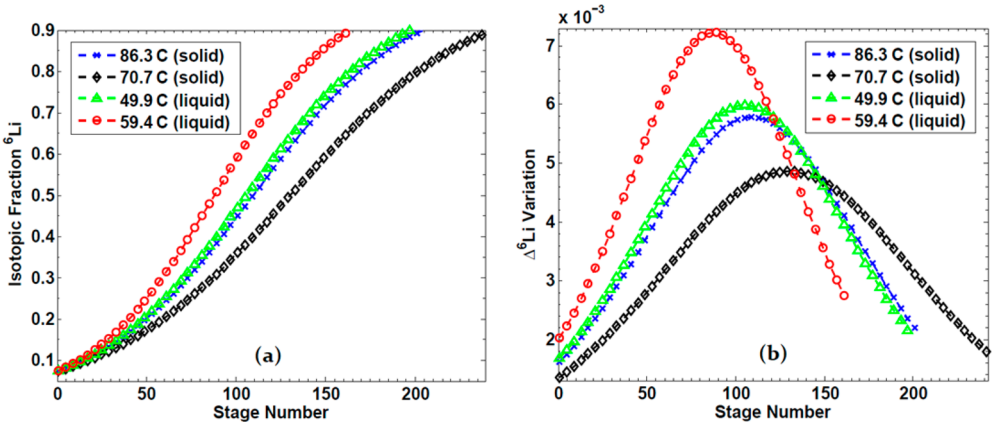

Figure 6. Simulation results for the electrochemical insertion of lithium into gallium: (a) enrichment curve per stage and (b) ^{6}Li isotopic fraction variation per stage.

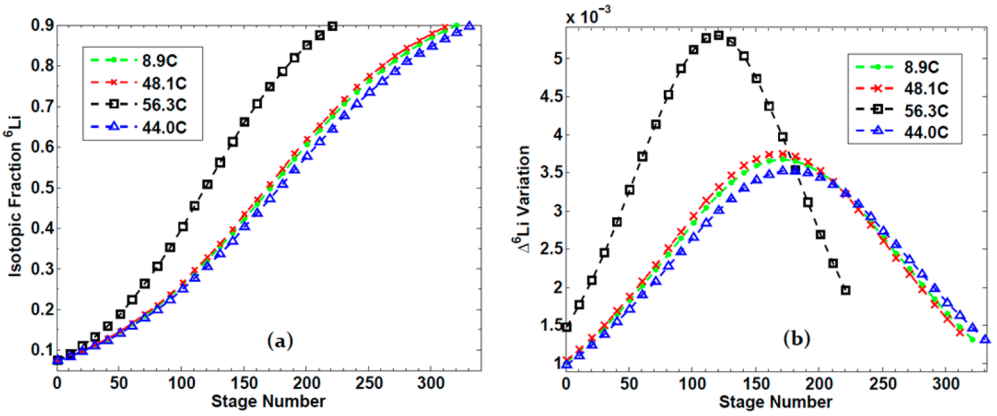

Figure 7. Simulation results for the electrochemical insertion into zinc method for isotopes Li separation: (a) enrichment curve per stage and (b) ^{6}Li isotopic fraction variation per stage.

higher cost for the electrode material. The electrochemical intercalation reaction is depicted in eq 16:

$$\mathrm{Ga} + n\mathrm{Li}^{+} + n\mathrm{e}^{-} \leftrightarrow \mathrm{Li}_{n}\mathrm{Ga} \tag{16}$$

The reported cell consists of a high-purity gallium cathode working below the melting temperature, or, alternatively, in a compartment that contains 5−12 g of liquid gallium with a relatively high contact surface area (0.78 cm^2) with the electrolyte solution. In the liquid phase, the classical ethylene carbonate (EC) and methylethyl carbonate (MEC) mixture containing $LiClO_4$ is used. In the case of the solid gallium, experiments with 1 M LiCl in dimethyl sulfoxide have also been reported. Lithium foils were used both as counter and reference electrodes. An in−out diagram is depicted in Figure 2d. The electrochemical cell is constructed in a three-electrode configuration for the measurements. The electrolysis is conducted in a constant current mode first, until the electrode potential reaches the 0.02 V value. From this point, the working mode is changed to constant voltage mode, until reaching a predetermined total charge value.

In Figure 6a, results for the simulation of ^{6}Li enrichment value are plotted versus stage number. Figure 6b shows the associated ^{6}Li isotopic difference in the gallium cathode. It is observed that the best performance is achieved with a liquid gallium cathode, and with the highest value of total charge tested. Table S4 in the Supporting Information summarize all our results for the simulations, as well as representative data from the original work.

No correlation is observed in a graph of the stoichiometric number n and the α value. In a first analysis, this would indicate that the isotopic separation is not dependent on the amount of lithium intercalated, at least for the quantities tested by Zenzai et al. No correlation is found either for insertion time, or current efficiency. The reversibility of the electrochemical intercalation process was studied by Tarascon et al.[63] Unfortunately, the very attractive lithium insertion capacity of gallium is associated with cyclability issues, which, in turn, are caused by the Li-driven large volume changes.

The α value is associated with the equilibrium constant of the isotopic exchange reaction,

$$^{7}\mathrm{Li(Ga)} + {}^{6}\mathrm{Li}^{+}_{(sol)} \leftrightarrow {}^{6}\mathrm{Li(Ga)} + {}^{7}\mathrm{Li}^{+}_{(sol)} \tag{17}$$

The equilibrium constant can be estimated as the reduced partition function ratio using molecular orbital theory to calculate the vibrational frequency of the stable species on the electrolyte and in the cathode. Results obtained by Zenkai et al.[47,48] are not in complete agreement with the experimental result, indicating that other causes may be responsible for the relatively large isotopic effect.

We see the insertion of Li^{+} ions into gallium as an elegant approach for the isotopic separation. However, issues with volume changes might determine that the full alloying capacity (up to 2 mol of Li atoms per mole of Ga atoms) might not be

DOI: 10.1021/acs.iecr.8b01640
Ind. Eng. Chem. Res. XXXX, XXX, XXX−XXX

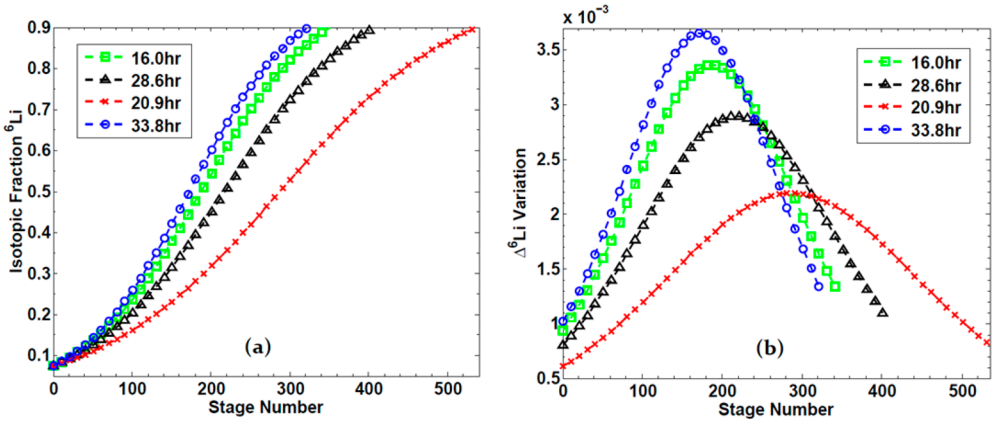

Figure 8. Simulation results for the electrochemical insertion of lithium into tin: (a) enrichment curve per stage and (b) ^{6}Li isotopic fraction variation per stage.

fully exploitable. A full economic analysis is also mandatory, in view of the clear differential costs when comparing insertion into gallium or graphite, particularly if we consider that the full insertion capacity of gallium might not be usable to our advantage.

3.5. Electrochemical Insertion into Zinc. Another possibility as host material for lithium electrochemical insertion is zinc, which is an interesting alternative because of its abundance, price, and nontoxicity, and the existence of Li−Zn alloys has been well-studied.[64] In this context, Mouri et al.[49] reported the isotopic separation associated with reaction 18.

$$n\mathrm{Li}^+ + n\mathrm{e}^- + \mathrm{Zn} \leftrightarrow \mathrm{Li}_n\mathrm{Zn} \quad (18)$$

Figure 2e depicts an in−out diagram for the proposed separation system. The lithium sample to be enriched is the common $LiClO_4$ solution in an EC/MEC solvent mixture. The solid zinc−lithium alloy is enriched in ^{6}Li. The electrochemical reported reactor is a three-electrode system, consisting of additional lithium foils as both counter and reference electrodes, in addition to the zinc cathode. Lithium insertion is performed in an initial constant current (1−5 mA), followed by a constant voltage (0.02 V) mode. The electrolysis is continued until the total charge delivered achieves different values (see Figure 7). Figure 7a depicts our calculations for the evolution of the ^{6}Li fraction in the Zn−Li alloys throughout an entire cascade process for six selected runs. The shorter fractionation overall process corresponds to the largest amount of lithium inserted (highest total charge value, 56.3 C). In addition, a correlation is observed between the stoichiometric factor in the final cathode composition (n) and the separation factor (α),[49] which is indeed very convenient, in view of future scale-up activities. Figure 7b depicts the corresponding isotopic difference curve versus the stage number. Table S5 in the Supporting Information summarizes all of our results for the simulations, as well as representative data from the original work.

Scanning electron microscopy (SEM) and X-ray diffraction (XRD) analysis verified the formation of the Li−Zn alloys both in the surface of different types of zinc cathodes and the diffusion process toward the cathode core. In previous work, the life cycle of Li−Zn alloys was studied.[64] A better performance was obtained by the addition of inert materials (Fe) at the cathode.

3.6. Electrochemical Insertion of Lithium into Tin. The last material that has been evaluated for lithium insertion was metallic tin. The methodology was developed by Yanase et al.[50] Tin compounds have been reported as an alternative to graphite in lithium-ion anodes.[65−67] Various different phases and stoichiometric structures for Li−Sn alloys have been reported. A general chemical reaction is given in reaction 19:

$$n\mathrm{Li}^+ + x\mathrm{e}^- + \mathrm{Sn} \leftrightarrow \mathrm{Li}_n\mathrm{Sn} \quad (19)$$

The reported experimental reactor consists of a three-electrode arrangement. A tin metal wire is used as a cathode, while lithium foils are used as both counter and reference electrode. The electrolyte was a 1 M solution of $LiPF_6$ in a mixture of EC and MEC. An in−out diagram is shown in Figure 2g. The reactor was first operated in constant current mode (1 mA), until a certain voltage was reached, and from that point on, the electrolysis continued in constant voltage mode until the total charge reached a value of 28.08 C.

The enrichment curved for the entire cascade process are depicted in Figure 8a, and the corresponding isotopic difference curve are shown in Figure 8b. Table S6 in the Supporting Information summarizes all of our results for the simulations, as well as representative data from the original work.

The most efficient operation mode corresponds to the experiment where the constant current mode was kept until a voltage of 0.3 V that was then kept constant. The total electrolysis time for that experiment was of 33.8 h, and a current efficiency of 64% was reported.

3.7. Isotope Separation by Electrodialysis through Embedded Organic Membrane with Ionic Liquid. This technique takes advantage of the different ionic mobilities of ^{6}Li$^+$ and ^{7}Li$^+$ cations through an ionic-liquid-impregnated organic membrane located between the cathode and anode compartment of an electrodialysis cell. In this cell, water is both oxidized and reduced at platinum inert electrodes, and the passage of lithium cations through the membrane is necessary to keep the electroneutrality of the anodic and cathodic compartments.[51,52] A highly porous Teflon membrane embedded in PP13-TSFI (ionic liquid) separates the cell into two compartments, whereby flows a solution with an equimolar mixture of LiCl and NaCl.

This method present maximum values of isotopic separation ~8 and ~10 times larger than the other techniques; as a consequence, it is not surprising that the number of times that

DOI: 10.1021/acs.iecr.8b01640
Ind. Eng. Chem. Res. XXXX, XXX, XXX−XXX

we have to repeat the process will be much less than the other methods. The isotopic separation efficiency is inversely proportional to the applied current density. We certainly like the idea of working in aqueous media, as opposed to anhydrous solutions and anoxic conditions. However, we must admit that we are very puzzled at the unusually high separation efficiencies reported by the authors. The reported enrichment factors (ε = 0.1−0.4) are ∼1 order of magnitude higher than those for other techniques reported here, as well as for the currently employed large-scale technology for separation of lithium isotopes, formation of lithium−mercury amalgams (ε = 0.049−0.062).[68] Calculations do indeed show that the isotope effect—and, hence, the separation coefficient—should be slightly larger in aqueous media than in organic media.[68,69] However, we have not found a suitable explanation for the astoundingly large increase in separation factor reported by these authors, compared to that of lithium amalgamation in mercury. In addition, we are worried about the instability of the ionic liquid, in which the membrane is embedded, with no specific chemical attachment or physical entrapment. It is reported by the authors themselves that, under the influence of the potential difference, the ionic liquid molecules tend to migrate. Obviously, this decrease in ionic liquid composition affects the separation performance, since it is reported that the ionic mobility of ^{6}Li and ^{7}Li will be similar through the organic membrane without the ionic liquid molecules. The authors also report the dependency of isotope separation factor versus the loss of ionic liquid. Note that the worst separation performance and larger losses of ionic liquid occur for the larger current density values.

Therefore, our calculations are based on data over which we have serious questions. The enrichment curve for the entire cascade process is depicted in Figure S1a in the Supporting Information, and the corresponding isotopic difference curve is shown in Figure S1b in the Supporting Information. Because of the unusually high α values, for the best possible scenario, the desired 90% enrichment in ^{6}Li is achieved after, surprisingly, only 16 stages. Table S7 in the Supporting Information summarizes all of our results for the simulations, as well as representative data from the original work.

4. DISCUSSION

In all of the work analyzed here, results are focused on the enrichment in ^{6}Li. The authors of the original experimental work did focus their work on the enrichment in the lighter isotope, and we have run the simulations focusing on the recuperation of the lightest isotope preferentially. A first conclusion of most enrichment experiments analyzed is the observation that the mass of the enriched phase is negligible, compared to the initial mass of reactants. This is observed in Table 1, where we show the percentage of the lithium ions present in the original phase that have been transferred to the enriched phase. The clear exception is delithiation of the LMO electrode (see section 3.3 above), where over a quarter of the original lithium presented in the original phase is transferred to the enriched phase. For all other examples, although the initial phase is enriched in the heavier isotope (^{7}Li), in practical terms, the relative compositions of ^{7}Li and ^{6}Li in the initial phase can be considered to remain invariable, because of the small fraction of ions that have been transferred. This fact requires important modifications to the base methodology if we wish to simultaneously recover samples enriched in both ^{6}Li and ^{7}Li, and these modifications are synonymous with a multiplication of separation stages. However, we must highlight that, in theory, these techniques could alternatively be used to prepare samples enriched in either ^{6}Li or ^{7}Li. However, for the purpose of recovering ^{7}Li-enriched samples, the methodology should be performed until most of the mass of the initial phase has been consumed, and, in this case, the enriched phase will be the initial phase.

The algorithm that we have developed can be equally used to calculate the number of stages needed to enrich a sample in ^{7}Li. However, since the experimental data used to feed the simulations only provided experimental results for the α enrichment factor in ^{6}Li, we, instead, focused our work on this isotope. For better accuracy, it would be ideal to have experimental data for the α enrichment factor in ^{7}Li, which does not necessarily have the same numerical value as its analogue for ^{6}Li.

There are several important issues to analyze upon thinking of a scale-up process of a technique that has been successfully proven at laboratory scale. In our particular case, we are very much concerned that several of the analyzed articles couple the reaction of interest for isotopic enrichment with a counter electrode where metallic lithium is oxidized to lithium cations.[45,47−50] This reaction is simple and most interesting from the perspective of not introducing species into the solution that might be difficult to separate later. However, it is evident to us that there will be an isotopic effect associated with this electrochemical reaction as well. And, as a consequence, this reaction, in turn, will produce an isotopic enrichment, both in the metallic phase and in the solution phase. It is very surprising that none of the experimental articles that were reported to have used this counter electrode have mentioned this possibility. We do not have sound experimental evidence to assert undoubtedly which of the two isotopes will preferentially remain in the solid phase and which one will preferentially migrate to solution upon oxidation of a metallic lithium electrode, although we have several pieces of information that strongly suggest the expected partition. First, there is large experimental evidence that, upon electroplating different metals such as lithium,[44] zinc,[70] iron[71] and copper,[72,73] the metallic phase is always enriched in the lightest isotope. Moreover, we have also seen, in the work analyzed, that the lightest isotopologue is always deposited preferentially in the solid phase. Finally, Yanase and Oi[68,69] made molecular orbital calculations for the two lithium isotopes in combination with several dozen elements of the periodic table. They calculated the frequency shifts upon ^{7}Li/^{6}Li substitution and the isotopic reduced partition function ratio (rpfr). For absolutely all analyzed compounds, they did show a preferential partition of the lighter isotope in the solid face versus its heavier isotopologue, albeit of different magnitude.

Overall, although no experiments have been reported, it is very reasonable to hypothesize that upon oxidation of metallic lithium at the counter electrode, the solid phase will become enriched in ^{6}Li, while the oxidized ions will show a preferential composition of ^{7}Li. All articles analyzed pay attention exclusively to the isotopic enrichment generated at the cathode. In light of a very likely electrochemical isotope effect at the metallic lithium electrode (anode), we expect that the total isotopic composition will be affected. At later stages, when the departing phase is already heavily enriched in ^{6}Li, we certainly do not want that a metallic anode with the natural isotope composition that will liberate ^{7}Li cations preferentially.

DOI: 10.1021/acs.iecr.8b01640
Ind. Eng. Chem. Res. XXXX, XXX, XXX−XXX

In addition, an interesting hypothesis to verify in view of scale-up possibilities would be to try to pursue the electrochemical process to produce higher cuts. For example, cut values of 5%−10% should be small enough to still produce an isotopic enrichment, but high enough to produce a detrimental influx of ^{7}Li in the liquid phase from the anode. In addition, even if we disregard the isotope effect at the counter electrode, if this electrode is made out of nonenriched metallic lithium, it will still liberate ^{7}Li preferentially, because this is much more abundant than ^{6}Li in a natural sample. And once again, this is undesirable in the intermediate and late stages, when the feed solution is already heavily enriched in ^{6}Li.

The next topic to analyze, in view of prospective scale-up possibilities, is the overall context of the different proposed methodologies. We would be dealing with methodologies that would require, in any case, repetition of the basic operational process over a hundred times. Hence, it is important to consider how to reset the initial reaction conditions, to proceed with the successive stage, i.e., how to back-extract the lithium from the different enriched phases (most often, the solid phase). For example, the question arises as to how to transform an isotopically enriched lithium metallic sample (i.e., the head in the process described above in section 3.1) into a $LiClO_4$ 1 M solution with the same isotopic composition as that lithium metallic sample. We need to keep the same isotopic composition of the head of stage n, in the feed of stage $n + 1$. This procedure should be straightforward, since it will have to be repeated as many times as the number of stages necessary in the overall process. In this context, all the methodologies where the enriched sample is produced in a solid phase, at a cathode, metallic lithium deposition, and intercalation in graphite, gallium, tin, or zinc, seem to show an advantage versus the other methodologies. In principle, for those methodologies, it should be possible to recover all the enriched lithium ions by reverting the potential or current, and dissolving back all the lithium into a fresh solution, which can be directly used as a departing solution in the consecutive stage. Conversely, it is clearly not as straightforward to think of a fast and efficient way to prepare LMO enriched in ^{6}Li that is found in solution, in a series of up to 250 stages.

The situation seems even more complicated in the case of the work presented by Hoshino and Terai.[51,52] In that work, the enriched lithium sample is observed to be mixed with larger amounts of NaCl, while the departing material for the consecutive stage should be a pure LiCl solution. Separation of LiCl from NaCl is a very well-studied topic, since Li_2CO_3 from brines is extracted from natural brines, which have a molecular ratio of ∼40:1 in Na:Li.[74−76] The most common technique—evaporation and sequential precipitation—certainly does not seem applicable, because of space, time, and weather issues. Other separation methodologies are not easy, and their implementation in a cascade process for at least 13 times does not seem straightforward.

In addition, Table 1 also gathers representative data from the original research articles, such as Coulombic efficiency of the process, total charge per stage in the reported results, and cut values, i.e., percentage of the original total lithium that underwent through the electrochemical process (electrodeposition, insertion, etc.). Note the very low Coulombic efficiency of the electrodeposition process. This is an issue to be resolved, since a low Coulombic efficiency is synonymous with being a waste of money. In addition, the environmental costs of reducing large amounts of organic solvents and/or ClO_4^- (the only possible parallel reactions) should be evaluated. Moreover, an evaluation should also be performed to characterize the decomposition products, and determine if these will interfere in the further electrochemical processing of the $LiClO_4$ organic solutions. Although not ideal, we could potentially consider to discard the remaining solution after the first stage of a process. However, we certainly cannot discard $LiClO_4$ organic solutions that are already enriched in ^{6}Li, even though the desired 90% (or whatever enrichment value is sought) has not yet been reached, because this solution contains large amounts of decomposition products that are detrimental to the overall process. In this respect, intercalation of lithium into graphite, gallium, and zinc showed considerably higher Coulombic efficiency values.

Table 1 is a summary of our calculations (minimum number of stages needed, energy consumption and costs) and the most relevant information provided in the original experimental articles, for the different analyzed methodologies. It is important to highlight that the electrical consumption and the consequent electricity costs have been calculated only for the electrochemical stages of the isotopic separation process. Our calculation does not take into account any other associated steps that are surely going to be required for a full or pilot scale process, such as purification or drying of the reactants, or the transformation of the deposited metallic lithium, or intercalated lithium, into a lithium salt for the consecutive enrichment stages. In addition, the energy consumption was calculated assuming the prospective industrial or pilot process has already reached a steady state. We have already mentioned that, in each enrichment stage, only a minor fraction of the total amount of lithium is transferred from the original phase to the enriched phase. This requires that a relatively large pool of reactants for each intermediate stage must be produced. This can be realized by either continuously repeating the earlier stages in batch mode several times to fill up the later stages, by dimensioning the earlier stages to larger capacity than later stages, and by cleverly combining the intermediate fluxes (see below), or by a combination of all of these processes. In any case, we are aware that there will be an important cost related to achieving a steady-state operating condition. Another point to be considered is the fact that studies are still needed to evaluate which is the maximum amount of material that can be transferred from one phase to another one, while keeping the maximum isotopic enrichment. In other words, for each of the analyzed methodologies, it is yet to be determined whether only the small reported fraction can be transferred to the enriched phase, or whether the amount of material transferred (relative to the total amount of lithium present) can be incremented.

It would have been interesting to compare results for the different proposed methodologies under the same operating conditions. However, this is not possible since only a restricted number of experiments have been reported in each of the original articles. On one hand, different methodologies are applied under different electrochemical conditions, either constant voltage (section 3.1), constant current (section 3.7), or constant current followed by constant voltage (sections 3.2−3.6). In addition, even those authors who have followed the same general operational mode have worked at considerably different current, voltage, or total charge values. Compare, for example, experiments in sections 3.2−3.6. Reported current values range from 1 mA to 3 mA, and

DOI: 10.1021/acs.iecr.8b01640
Ind. Eng. Chem. Res. XXXX, XXX, XXX−XXX

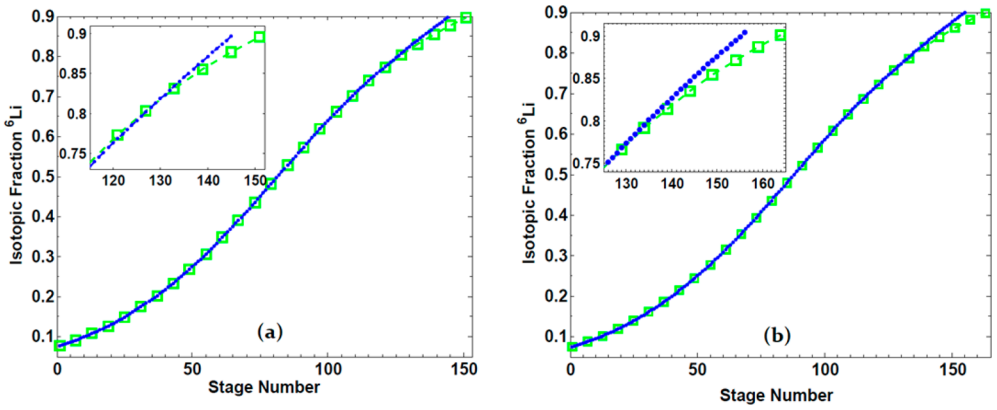

Figure 9. Comparison between simulations for the optimal operating condition (one unique operating condition, green line, squares), and a combination of different operation parameters (blue line, dots): (a) lithium electrodeposition and (b) lithium electrochemical insertion into gallium.

these current values are not normalized. Even much larger variations are reported for total current values. While some authors remain at low total currents (not beyond 4.16 C, section 3.3), others work between 50 C and 86 C (section 3.6). Tables S1−S7 in the Supporting Information list the detailed operating conditions of the original reports.

An analysis of the energy consumption shows relatively low prices for a prospective pilot or large-scale production of the ^{6}Li isotope via an electrochemical methodology, with values ranging from 2520 Wh g^{-1} to 6640 Wh g^{-1}. The cost analysis, combined with high Coulombic efficiencies, in addition to the number of stages needed, certainly favors insertion into either gallium or graphite versus any of the other methodologies. However, we should still bear in mind that both reactor materials and electrodes, together with the energy costs of all side processes, will considerably add to the final cost of the overall process. In this respect, the overall cost balance might end up turning favorable toward any of the other processes, since the cost estimations at this preliminary stage are not enormously different (by a factor of <3).

Evidently, one of the assumptions considered throughout the calculations imply that we have available material with a wide range of isotopic composition to replenish the process streams upon requirement. This condition is achieved in real isotope separation systems through the recirculation of the head and tail fluxes of the same, or other stages. In Figure 1, it is visible that a large volume of materials with different isotopic composition are available for recycling from the intermediate fluxes. The development of this structure process and the interaction between fluxes and separation units is known as Cascade Theory.[2] The scientific literature is plentiful in work focused in the development and optimization of process topology.[77−79] A deep analysis on how to apply those concepts to the present examples is unfortunately beyond the scope of the present article.

The attentive reader might have noticed the correlation between the panels from the left and those from the right in Figures 3−8. If we think that the total number of stages is quite large, we could consider the variable n, which denotes the number of stages, as a continuum, and, hence, the small gap between two consecutive stages could be considered as a differential. Under this assumption, and following the definition of enrichment grade between stages (eq 13), the curves plotted in Figures 3−8b can be considered the derivatives of the corresponding curves in Figures 3−8a. These derivative curves are the easiest way to spot immediately which of the working conditions (current value/voltage/total charge) will yield the highest possible enrichment for a given departing isotopic composition. From analyzing the isotopic difference curves (Figures 3−8b), we see that the maximum efficiency for the process is not always that achieved for the optimal conditions listed in Table 1. We observe that, for the early and medium stages, the efficiency is maximum for a given operating condition, but from a certain enrichment value onward, this is shifted to different operating conditions. For example, for the electrodeposition of metallic lithium, in order to reach an isotopic fraction of 0.5 in ^{6}Li, in order to employ the lowest possible number of stages, it is best to work at an overpotential of 0.06 V. In this way, the desired enrichment is reached after 82 stages. However, to reach higher isotopic enrichment fractions, from that point on, it is best to move sequentially to overpotentials of 0.01 and 0.13 V. In this way, a desired final isotopic fraction of 0.9 can be reached in 145 stages, instead of 153 total stages. This is depicted in Figure 9a, where the isotopic enrichment curve for a unique operating condition is plotted together with the curve for the combination of the conditions just discussed. A similar analysis can be made for any of the other electrochemical methodologies. As a second example, the case of the electrochemical insertion of lithium into gallium is depicted in Figure 9b. In this case, our calculations show that by combining different working conditions, we could save 7 stages, with the total number of stages being 156 (combination of operating conditions) versus 163 (using a total charge condition of 59.4 C). The combination of different operating conditions should be easy to implement and, in principle, would not require extra investment, since the electrochemical equipment used should be exactly equal to previous stages.

5. CONCLUSIONS

We have surveyed previous publications on prospective electrochemical technologies for stable lithium isotope separation. We have started from the experimental results in those publications, and we have calculated the amount of consecutive stages that would be needed to implement the proposed methodologies to reach a certain degree of enrichment. Our simulations were based in a series of assumptions, most importantly, that the enrichment factor is

DOI: 10.1021/acs.iecr.8b01640
Ind. Eng. Chem. Res. XXXX, XXX, XXX−XXX

maintained despite composition changes in the departing material. We also assume it is possible to reset the initial conditions.

Our simulations show that the technology requiring the least number of stages to reach a 90% enrichment is the electrodyalisis of an aqueous solution of LiCl through a membrane that has been previously embedded in an ionic liquid. However, we have expressed our serious doubts about the abnormally high enrichment factor reported by the authors of the original research, as well as experimental complications arising from the hypothetical large-scale implementation of this technology.

Other than electrodialysis, the electrodeposition of metallic lithium and insertion of lithium cations into gallium, with 153 and 163 stages, respectively, are the methodologies with more promising results. The former presents several advantages in view of a prospective scaling up, although a low Coulombic efficiency, which is due to solvent decomposition, is to be noted. The latter is an interesting technique, although the cost of gallium, and expansion of the electrode material upon lithium insertion, should be studied more carefully.

An estimation of the energy consumption has been made, showing values between 2290 and 6640 Wh g^{-1} for the production of samples with a 90% enrichment in ^{6}Li. Overall, in our opinion, no electrochemical technology has yet shown conclusive results to show clear advantages over competitive methodologies. Together with results from simulations, more experimental work is needed to allow engineers to decide upon which technology is worth testing for pilot scaling.

■ ASSOCIATED CONTENT

Supporting Information

The Supporting Information is available free of charge on the ACS Publications website at DOI: 10.1021/acs.iecr.8b01640.

Tables with summary of tested operating conditions, and results for Coulombic efficiencies as reported in the original articles; figure with calculations using data from refs 51 and 52 (PDF)

■ AUTHOR INFORMATION

Corresponding Author

*E-mail: vflexer@unju.edu.ar.

ORCID

Victoria Flexer: 0000-0002-4385-8846

Notes

The authors declare no competing financial interest.

■ ACKNOWLEDGMENTS

V.F. is a research fellow from CONICET. L.N.A. acknowledges a doctoral fellowship from CONICET. Funding from Agencia Nacional de Promoción Científica y Tecnológica, through Nos. PICT V-2014 3654 and FITR-INDUSTRIA 9/2013, are gratefully acknowledged.

■ REFERENCES

(1) Coplen, T. B.; Böhlke, J. K.; De Bièvre, P.; Ding, T.; Holden, N. E.; Hopple, J. A.; Krouse, H. R.; Lamberty, A.; Peiser, H. S.; Revesz, K.; Rieder, S. E.; Rosman, K. J. R.; Roth, E.; Taylor, P. D. P.; Vocke, R. D.; Xiao, Y. K. Isotope-Abundance Variations of Selected Elements (IUPAC Technical Report). *Pure Appl. Chem.* **2002**, *74*, 1987−2017.

(2) Wolfsberg, M.; VanHook, W. A.; Piotr, P. *Isotope Effects in the Chemical, Geological, and Bio Sciences*; Springer, Dordrecht, The Netherlands, 2010.

(3) Cartwright, I.; Cendón, D.; Currell, M.; Meredith, K. A Review of Radioactive Isotopes and Other Residence Time Tracers in Understanding Groundwater Recharge: Possibilities, Challenges, and Limitations. *J. Hydrol.* **2017**, *555*, 797−811.

(4) Fraile, L. M.; Herraiz, J. L.; Udías, J. M.; Cal-González, J.; Corzo, P. M. G.; España, S.; Herranz, E.; Pérez-Liva, M.; Picado, E.; Vicente, E.; Muñoz-Martín, A.; Vaquero, J. J. Experimental Validation of Gallium Production and Isotope-Dependent Positron Range Correction in PET. *Nucl. Instrum. Methods Phys. Res., Sect. A* **2016**, *814*, 110−116.

(5) Permana, S.; Novitrian; Ismail; Suzuki, M.; Saito, M. Analysis on Isotopic Plutonium Barrier Based on Spent Nuclear Fuel of LWR. *Ann. Nucl. Energy* **2015**, *75*, 116−122.

(6) Spano, T. L.; Simonetti, A.; Balboni, E.; Dorais, C.; Burns, P. C. Trace Element and U Isotope Analysis of Uraninite and Ore Concentrate: Applications for Nuclear Forensic Investigations. *Appl. Geochem.* **2017**, *84*, 277−285.

(7) Wen, B.; Zhou, J.; Zhou, A.; Liu, C.; Li, L. A Review of Antimony (Sb) Isotopes Analytical Methods and Application in Environmental Systems. *Int. Biodeterior. Biodegrad.* **2018**, *128*, 109−116.

(8) Niu, B.; Jin, L.; Li, Y.; Shi, Z.; Hu, H. Isotope Analysis for Understanding the Hydrogen Transfer Mechanism in Direct Liquefaction of Bulianta Coal. *Fuel* **2017**, *203*, 82−89.

(9) Sears, V. F. Neutron Scattering Lengths and Cross Sections. *Neutron News* **1992**, *3*, 26−37.

(10) Zinkle, S. J.; Busby, J. T. Structural Materials for Fission & Fusion Energy. *Mater. Today* **2009**, *12*, 12−19.

(11) Tanabe, T. Characteristics of Tritium. In *Tritium: Fuel of Fusion Reactors*; Springer: Tokyo, 2017; pp 27−48.

(12) Meija, J.; Coplen, T. B.; Berglund, M.; Brand, W. A.; De Bièvre, P.; Gröning, M.; Holden, N. E.; Irrgeher, J.; Loss, R. D.; Walczyk, T.; Prohaska, T. Isotopic Compositions of the Elements 2013 (IUPAC Technical Report). *Pure Appl. Chem.* **2016**, *88*, 293−306.

(13) Tobita, K.; Nishio, S.; Tanigawa, H.; Enoeda, M.; Isono, T.; Nakamura, H.; Tsuru, D.; Suzuki, S.; Hayashi, T.; Tsuchiya, K.; Hayashi, T.; Nishitani, T. Torus Configuration and Materials Selection on a Fusion DEMO Reactor, SlimCS. *J. Nucl. Mater.* **2009**, *386*−*388*, 888−892.

(14) Donne, M. D.; Anzidei, L.; Kwast, H.; Moons, F.; Proust, E. Status of EC Solid Breeder-Blanket Designs and R&D for DEMO Fusion Reactors. *Fusion Eng. Des.* **1995**, *27*, 319−336.

(15) Wang, W.; Julaiti, P.; Ye, G.; Huo, X.; Chen, J. Controlled Architecture of Macrocyclic Ligand Functionalized Polymer Brushes from Glass Fibers Using Surface-Initiated ICAR ATRP Technique for Adsorptive Separation of Lithium Isotopes. *Chem. Eng. J.* **2018**, *336*, 669−678.

(16) Xiao, J.; Jia, Y.; Shi, C.; Wang, X.; Wang, S.; Yao, Y.; Jing, Y. Lithium Isotopes Separation by Using Benzo-15-Crown-5 in Eco-Friendly Extraction System. *J. Mol. Liq.* **2017**, *241*, 946−951.

(17) Liu, Y.; Liu, F.; Ye, G.; Pu, N.; Wu, F.; Wang, Z.; Huo, X.; Xu, J.; Chen, J. Macrocyclic Ligand Decorated Ordered Mesoporous Silica with Large-Pore and Short-Channel Characteristics for Effective Separation of Lithium Isotopes: Synthesis, Adsorptive Behavior Study and DFT Modeling. *Dalt. Trans.* **2016**, *45*, 16492−16504.

(18) Trauger, D. B.; Keyes, J. J. J.; Kuipers, G. A.; Lang, D. M. Some Experiments on the Separation of Lithium Isotopes by Molecular Distillation. In *Proceedings of the Symposium on Isotope Separation*, Amsterdam, April 23−27, 1957; North-Holland: Amsterdam, 1957; Chapter 27.

(19) Shi, C.; Jia, Y.; Xiao, J.; Wang, X.; Yao, Y.; Jing, Y. Lithium Isotope Separation by Liquid-Liquid Extraction Using Ionic Liquid System Containing Dibenzo-14-Crown-4. *J. Mol. Liq.* **2016**, *224*, 662−667.

DOI: 10.1021/acs.iecr.8b01640
Ind. Eng. Chem. Res. XXXX, XXX, XXX−XXX

(20) Kim, D. W.; Jeon, Y. S.; Eom, T. Y.; Suh, M. Y.; Lee, C. H. Lithium Isotope Separation on a Monobenzo-15-Crown-5 Resin. *J. Radioanal. Nucl. Chem.* **1991**, *150*, 417−426.
(21) Yan, F.; Liu, H.; Pei, H.; Li, J.; Cui, Z.; He, B. Polyvinyl Alcohol-Graft-Benzo-15-Crown-5 Ether for Lithium Isotopes Separation by Liquid−solid Extraction. *J. Radioanal. Nucl. Chem.* **2017**, *311*, 2061−2068.
(22) Yan, F.; Pei, H.; Pei, Y.; Li, T.; Li, J.; He, B.; Cheng, Y.; Cui, Z.; Guo, D.; Cui, J. Preparation and Characterization of Polysulfone-Graft-4′-Aminobenzo-15-Crown-5-Ether for Lithium Isotope Separation. *Ind. Eng. Chem. Res.* **2015**, *54*, 3473−3479.
(23) Kim, D. W.; Hong, C. P.; Kim, C. S.; Jeong, Y. K.; Jeon, Y. S.; Lee, J. K. Lithium Isotope Separation on an Ion Exchange Resin Having Azacrown Ether as an Anchor Group. *J. Radioanal. Nucl. Chem.* **1997**, *220*, 229−231.
(24) Nishizawa, K.; Watanabe, H.; Ishino, S.-I.; Shinagawa, M. Lithium Isotope Separation by Cryptand (2B, 2, 1) Polymer. *J. Nucl. Sci. Technol.* **1984**, *21*, 133−138.
(25) Mikeš, J.; Ďurišová, J.; Jelínek, L. Enrichment of Lithium Isotope 6Li by Ion Exchange Resin with Specific Particle Size. *J. Radioanal. Nucl. Chem.* **2017**, *312*, 13−18.
(26) Kim, D. W.; Park, H. K.; Kim, C. S.; Jeon, Y. S. Separation of Lithium Isotopes with the N3O2 Trimerrifield Peptide Resin. *J. Radioanal. Nucl. Chem.* **1999**, *242*, 769−772.
(27) Kim, D. W. Separation of Lithium and Magnesium Isotopes by Hydrous manganese(IV) Oxide. *J. Radioanal. Nucl. Chem.* **2002**, *252*, 559−563.
(28) Takeuchi, H.; Oi, T.; Hosoe, M. Lithium Isotope Selectivity of Sorbents Prepared from Lithium Manganese Oxides. *Sep. Sci. Technol.* **1999**, *34*, 545−553.
(29) Kim, D. W.; Kang, B. M.; Jeon, B. K.; Jeon, Y. S. Separation of Lithium Isotopes by Elution Chromatography with an AB18C6 Bonded Merrifield Peptide Resin. *J. Radioanal. Nucl. Chem.* **2003**, *256*, 81−85.
(30) Fujine, S.; Saito, K.; Shiba, K. Lithium Isotope Separation by Displacement Chromatography Using Cryptand Resin. *J. Nucl. Sci. Technol.* **1983**, *20*, 439−440.
(31) Akimov, D. V.; Egorov, N. B.; Dyachenko, A. N.; Pustovalova, M. P.; Podoinikov, I. R. Lithium and Magnesium Isotopes Fractionation by Zone Melting. *IOP Conf. Ser.: Mater. Sci. Eng.* **2016**, *135*, 012001.
(32) Plekhanov, V. G. Isotope Effects on the Lattice Dynamics of Crystals. *Mater. Sci. Eng., R* **2001**, *35*, 139−237.
(33) Olivares, I. E.; Duarte, A. E.; Saravia, E. A.; Duarte, F. J. Lithium Isotope Separation with Tunable Diode Lasers. *Appl. Opt.* **2002**, *41*, 2973−2977.
(34) Arisawa, T.; Maruyama, Y.; Suzuki, Y.; Shiba, K. Lithium Isotope Separation by Laser. *Appl. Phys. B: Photophys. Laser Chem.* **1982**, *28*, 73−76.
(35) Saleem, M.; Hussain, S.; Rafiq, M.; Baig, M. A. Laser Isotope Separation of Lithium by Two-Step Photoionization. *J. Appl. Phys.* **2006**, *100*, 053111.
(36) Saleem, M.; Hussain, S.; Zia, M. A.; Baig, M. A. An Efficient Pathway for Li6 Isotope Enrichment. *Appl. Phys. B: Lasers Opt.* **2007**, *87*, 723−726.
(37) McInteer, B. B.; Potter, R. M. Nitric Oxide Distillation Plant for Isotope Separation. *Ind. Eng. Chem. Process Des. Dev.* **1965**, *4*, 35−42.
(38) McInteer, B. B. Isotope Separation by Distillation: Design of a Carbon-13 Plant. *Sep. Sci. Technol.* **1980**, *15*, 491−508.
(39) Hammerli, M.; Stevens, W. H.; Butler, J. P. Combined Electrolysis Catalytic Exchange (CECE) Process for Hydrogen Isotope Separation. In *Separation of Hydrogen Isotopes*; Rae, H. K., Ed.; ACS Symposium Series, No. *68*; American Chemical Society: Washington, DC, 1978; pp 110−125.
(40) Li, H. L.; Ju, Y. L.; Li, L. J.; Xu, D. G. Separation of Isotope 13C Using High-Performance Structured Packing. *Chem. Eng. Process.* **2010**, *49*, 255−261.
(41) Brooks, S.; Southworth, G. R. History of Mercury Use and Environmental Contamination at the Oak Ridge Y-12 Plant. *Environ. Pollut.* **2011**, *159*, 219−228.
(42) Okuyama, K.; Okada, I.; Saito, N. The Isotope Effects in the Isotope Exchange Equilibria of Lithium in the Amalgam-Solution System. *J. Inorg. Nucl. Chem.* **1973**, *35*, 2883−2895.
(43) Fujie, M.; Fujii, Y.; Nomura, M.; Okamoto, M. Isotope Effects in Electrolytic Formation of Lithium Amalgam. *J. Nucl. Sci. Technol.* **1986**, *23*, 330−337.
(44) Black, J. R.; Umeda, G.; Dunn, B.; McDonough, W. F.; Kavner, A. Electrochemical Isotope Effect and Lithium Isotope Separation. *J. Am. Chem. Soc.* **2009**, *131*, 9904−9905.
(45) Yanase, S.; Hayama, W.; Oi, T. Lithium Isotope Effect Accompanying Electrochemical Intercalation of Lithium into Graphite. *Z. Naturforsch., A: Phys. Sci.* **2003**, *58*, 306−312.
(46) Okano, K.; Takami, Y.; Yanase, S.; Oi, T. Lithium Isotope Effects upon Electrochemical Release from Lithium Manganese Oxide. *Energy Procedia* **2015**, *71*, 140−148.
(47) Zenzai, K.; Yanase, S.; Zhang, Y.-H.; Oi, T. Lithium Isotope Effect Accompanying Electrochemical Insertion of Lithium into Gallium. *Prog. Nucl. Energy* **2008**, *50*, 494−498.
(48) Zenzai, K.; Yasui, A.; Yanase, S.; Oi, T. Lithium Isotope Effect Accompanying Electrochemical Insertion of Lithium into Liquid Gallium. *Z. Naturforsch., A: Phys. Sci.* **2010**, *65*, 461−467.
(49) Mouri, M.; Yanase, S.; Oi, T. Observation of Lithium Isotope Effect Accompanying Electrochemical Insertion of Lithium into Zinc. *J. Nucl. Sci. Technol.* **2008**, *45*, 384−389.
(50) Yanase, S.; OI, T.; Hashikawa, S. Observation of Lithium Isotope Effect Accompanying Electrochemical Insertion of Lithium into Tin. *J. Nucl. Sci. Technol.* **2000**, *37*, 919−923.
(51) Hoshino, T.; Terai, T. Basic Technology for ^{6}Li Enrichment Using an Ionic-Liquid Impregnated Organic Membrane. *J. Nucl. Mater.* **2011**, *417*, 696−699.
(52) Hoshino, T.; Terai, T. High-Efficiency Technology for Lithium Isotope Separation Using an Ionic-Liquid Impregnated Organic Membrane. *Fusion Eng. Des.* **2011**, *86*, 2168−2171.
(53) Saito, S.; Takami, Y.; Yoshizawa-Fujita, M.; Yanase, S.; Oi, T. Lithium Isotope Effects upon Electrochemical Lithium Insertion to Host Material from Ionic Liquid Medium. *Prog. Nucl. Energy* **2011**, *53*, 999−1004.
(54) Okada, I.; Saito, N. Enrichment of Li-6 by Countercurrent Electromigration with Molten $LiNO_3$−NH_4NO_3 System. *J. Nucl. Sci. Technol.* **1974**, *11*, 314−316.
(55) Imai, M. Isotope Effects of Lithium Ions in Electromigration in Aqueous Solutions. *J. Inorg. Nucl. Chem.* **1975**, *37*, 123−126.
(56) Pletcher, D.; Walsh, F. C. *Industrial Electrochemistry*, Second Edition; Springer: Dordrecht, The Netherlands, 1990.
(57) Kruesi, W. H.; Fray, D. J. The Electrowinning of Lithium from Chloride-Carbonate Melts. *Metall. Trans. B* **1993**, *24*, 605−615.
(58) Black, J. R.; John, S. G.; Kavner, A. Coupled Effects of Temperature and Mass Transport on the Isotope Fractionation of Zinc during Electroplating. *Geochim. Cosmochim. Acta* **2014**, *124*, 272−282.
(59) Levi, M. D.; Aurbach, D. Simultaneous Measurements and Modeling of the Electrochemical Impedance and the Cyclic Voltammetric Characteristics of Graphite Electrodes Doped with Lithium. *J. Phys. Chem. B* **1997**, *101*, 4630−4640.
(60) Hashikawa, S.; Yanase, S.; Oi, T. Lithium Isotope Effect Accompanying Chemical Insertion of Lithium into Graphite. *Z. Naturforsch., A: Phys. Sci.* **2002**, *57*, 857−862.
(61) Thackeray, M. M.; Johnson, C. S.; Vaughey, J. T.; Li, N.; Hackney, S. A. Advances in Manganese-Oxide "composite" Electrodes for Lithium-Ion Batteries. *J. Mater. Chem.* **2005**, *15*, 2257−2267.
(62) Lide, D. R. *CRC Handbook of Chemistry and Physics*, 88th Edition; CRC Press: Boca Raton, FL, 2008.
(63) Saint, J.; Morcrette, M.; Larcher, D.; Tarascon, J. M. Exploring the LiGa Room Temperature Phase Diagram and the Electrochemical Performances of the Li_xGa_y Alloys vs. Li. *Solid State Ionics* **2005**, *176*, 189−197.

DOI: 10.1021/acs.iecr.8b01640
Ind. Eng. Chem. Res. XXXX, XXX, XXX−XXX

(64) Fujieda, T.; Takahashi, S.; Higuchi, S. Cycling Behaviour of Electrodeposited Zinc Alloy Electrode for Secondary Lithium Batteries. *J. Power Sources* **1992**, *40*, 283−289.
(65) Idota, Y.; Kubota, T.; Matsufuji, A.; Maekawa, Y.; Miyasaka, T. Tin-Based Amorphous Oxide: A High-Capacity Lithium-Ion-Storage Material. *Science (Washington, DC, U. S.)* **1997**, *276*, 1395−1397.
(66) Winter, M.; Besenhard, J. O. Electrochemical Lithiation of Tin and Tin-Based Intermetallics and Composites. Electrochim. *Electrochim. Acta* **1999**, *45*, 31−50.
(67) Han, J.; Kong, D.; Lv, W.; Tang, D. M.; Han, D.; Zhang, C.; Liu, D.; Xiao, Z.; Zhang, X.; Xiao, J.; He, X.; Hsia, F.-C.; Zhang, C.; Tao, Y.; Golberg, D.; Kang, F.; Zhi, L.; Yang, Q.-H. Caging Tin Oxide in Three-Dimensional Graphene Networks for Superior Volumetric Lithium Storage. *Nat. Commun.* **2018**, *9*, 402.
(68) Yanase, S.; Oi, T. Solvation of Lithium Ion in Organic Electrolyte Solutions and Its Isotopie Reduced Partition Function Ratios Studied by ab Initio Molecular Orbital Method. *J. Nucl. Sci. Technol.* **2002**, *39*, 1060−1064.
(69) Yanase, S.; Oi, T. Periodicity in ^{6}Li-to-^{7}Li Isotopic Reduced Partition Function Ratios of Diatomic Lithium Compounds. *J. Nucl. Sci. Technol.* **2005**, *42*, 362−367.
(70) Kavner, A.; John, S. G.; Sass, S.; Boyle, E. A. Redox-Driven Stable Isotope Fractionation in Transition Metals: Application to Zn Electroplating. *Geochim. Cosmochim. Acta* **2008**, *72*, 1731−1741.
(71) Black, J. R.; Young, E. D.; Kavner, A. Electrochemically Controlled Iron Isotope Fractionation. *Geochim. Cosmochim. Acta* **2010**, *74*, 809−817.
(72) Black, J. R.; John, S.; Young, E. D.; Kavner, A. Effect of Temperature and Mass Transport on Transition Metal Isotope Fractionation during Electroplating. *Geochim. Cosmochim. Acta* **2010**, *74*, 5187−5201.
(73) Black, J. R.; Crawford, J. A.; John, S.; Kavner, A. Redox Driven Stable Isotope Fractionation. In *Aquatic Redox Chemistry*; Tratnyek, P. G., Grundl, T. J., Haderlein, S. B., Eds.; ACS Symposium Series, No. *1071*; American Chemical Society: Washington, DC, 2011; pp 345−359 ().
(74) Choubey, P. K.; Kim, M.; Srivastava, R. R.; Lee, J.; Lee, J.-Y. Advance Review on the Exploitation of the Prominent Energy-Storage Element: Lithium. Part I: From Mineral and Brine Resources. *Miner. Eng.* **2016**, *89*, 119−137.
(75) Talens Peiró, L.; Villalba Méndez, G.; Ayres, R. U. Lithium: Sources, Production, Uses, and Recovery Outlook. *JOM* **2013**, *65*, 986−996.
(76) Swain, B. Recovery and Recycling of Lithium: A Review. *Sep. Purif. Technol.* **2017**, *172*, 388−403.
(77) Zeng, S.; Cheng, L.; Jiang, D.; Borisevich, V. D.; Sulaberidze, G. A. A Numerical Method of Cascade Analysis and Design for Multi-Component Isotope Separation. *Chem. Eng. Res. Des.* **2014**, *92*, 2649−2658.
(78) Zhang, Y.; Zeng, S.; Jiang, D.; Borisevich, V.; Sulaberidze, G. Further Optimization of Q-Cascades. *Chem. Eng. Res. Des.* **2015**, *100*, 509−517.
(79) Smirnov, A. Y.; Sulaberidze, G. A.; Xie, Q.; Borisevich, V. D. Design of Cascade with Locally Enlarged Flow for Enrichment of Intermediate Components of Multi-Isotope Mixtures. *Chem. Eng. Res. Des.* **2015**, *95*, 47−54.

DOI: 10.1021/acs.iecr.8b01640
Ind. Eng. Chem. Res. XXXX, XXX, XXX−XXX